Neuropharmacology 92 (2015) 69–79

Contents lists available at ScienceDirect

Neuropharmacology

journal homepage: www.elsevier.com/locate/neuropharm

Cannabinoid agonists rearrange synaptic vesicles at excitatory synapses and depress motoneuron activity *in vivo*

Victoria García-Morales [1], Fernando Montero [1], Bernardo Moreno-López*

Grupo de Neurodegeneración y Neuroreparación (GRUNEDERE), Área de Fisiología, Facultad de Medicina, Universidad de Cádiz, Cádiz, Spain

ARTICLE INFO

Article history:
Received 26 September 2014
Received in revised form
14 December 2014
Accepted 30 December 2014
Available online 13 January 2015

Keywords:
CB1 receptors
AMPAergic neurotransmission
Short-term depression
Hypoglossal motoneurons
Depolarization-induced suppression of excitation

ABSTRACT

Impairment of motor skills is one of the most common acute adverse effects of cannabis. Related studies have focused mainly on psychomotor alterations, and little is known about the direct impact of cannabinoids (CBs) on motoneuron physiology. As key modulators of synaptic function, CBs regulate multiple neuronal functions and behaviors. Presynaptic CB1 mediates synaptic strength depression by inhibiting neurotransmitter release, via a poorly understood mechanism. The present study examined the effect of CB agonists on excitatory synaptic inputs incoming to hypoglossal motoneurons (HMNs) *in vitro* and *in vivo*. The endocannabinoid anandamide (AEA) and the synthetic CB agonist WIN 55,212-2 rapidly and reversibly induced short-term depression (STD) of glutamatergic synapses on motoneurons by a presynaptic mechanism. Presynaptic effects were fully reversed by the CB1-selective antagonist AM281. Electrophysiological and electron microscopy analysis showed that WIN 55,212-2 reduced the number of synaptic vesicles (SVs) docked to active zones in excitatory boutons. Given that AM281 fully abolished depolarization-induced depression of excitation, motoneurons can be feasible sources of CBs, which in turn act as retrograde messengers regulating synaptic function. Finally, microiontophoretic application of the CB agonist O-2545 reversibly depressed, presumably via CB1, glutamatergic inspiratory-related activity of HMNs *in vivo*. Therefore, evidence support that CBs, via presynaptic CB1, induce excitatory STD by reducing the readily releasable pool of SVs at excitatory synapses, then attenuating motoneuron activity. These outcomes contribute a possible mechanistic basis for cannabis-associated motor performance disturbances such as ataxia, dysarthria and dyscoordination.

1. Introduction

Acute adverse effects of cannabis and synthetic cannabinoids (CBs), which elicit cannabimimetic effects similar to Δ9-tetrahydrocannabinol (the primary psychoactive constituent in cannabis) include hyperemesis syndrome, impaired coordination and performance, hypomotility, analgesia, catalepsy, anxiety, suicidal ideations/tendencies, and psychotic symptoms (Castaneto et al., 2014; Karila et al., 2014). Much information exists on CBs-mediated psychotropic effects such as anxiety, depression, reward, cognition, learning, and memory (Crane et al., 2013). However, less attention has been paid to the cellular and molecular mechanisms underlying impairment of motor skills, one of the most common acute adverse effects of cannabis (Hall and Degenhardt, 2009). Most such studies have focused on psychomotor effects of CBs (Castaneto et al., 2014; Crane et al., 2013; Roser et al., 2009; Wiley et al., 2014), but little is known about the direct impact of CBs on motoneuron physiology. A direct impact on motoneuron activity could be the underpinning, at least in part, of cannabis-induced alterations in motor performance (ataxia, dysarthria, and dyscoordination). Along this line, a depressing action by endocannabinoids (eCBs) on glycinergic synaptic transmission affecting spinal (El Manira et al., 2008) and bulbar motoneurons (Lozovaya et al., 2011; Mukhtarov et al., 2005) has been reported to date. However, little is known about the influence of CBs on the determinant glutamatergic drive arriving to motoneurons and how it affects their activity pattern.

eCBs, mainly arachidonoyl ethanolamide (Anandamide, AEA) and 2-arachidonoyl glycerol (2-AG), are lipid messengers that, as key modulators of synaptic function, regulate multiple neuronal functions and behaviors. eCBs are important mediators of short- and long-term synaptic plasticity. CB1, the most prevalent CB

* Corresponding author. Área de Fisiología, Facultad de Medicina, Plaza Falla, 9, 11003 Cádiz, Spain. Tel./fax: +34 956 015248.
E-mail address: bernardo.moreno@uca.es (B. Moreno-López).
[1] These two authors have contributed equally to this work.

http://dx.doi.org/10.1016/j.neuropharm.2014.12.036
0028-3908/

receptor in the brain, mediates a dominant form of inhibiting neurotransmitter release from presynaptic terminals (Kano et al., 2009). CB1 agonist activation triggers a cascade of reactions that affect cellular signaling and neurotransmitter inhibition, including acetylcholine, dopamine, noradrenaline, glutamine, and γ-aminobutyric acid (Mechoulam and Parker, 2013; Pertwee, 2010). Activated neurons produce eCBs that diffuse as retrograde messengers and bind to presynaptic CB1, which triggers transient Ca^{2+} channel inhibition and/or K^{+} channel activation, reducing the release probability of synaptic vesicles (SVs) (Castillo et al., 2012; Chevaleyre et al., 2006). The size of the readily releasable pool (RRP) of SVs is an important determinant of synaptic strength, short-term plasticity, and inter-synaptic crosstalk (Dobrunz, 2002; Gonzalez-Forero et al., 2012; Millar et al., 2002). Relative to presynaptic alterations, short-term forms of synaptic depression are usually attributed to depletion of some RRP of SVs (Schneggenburger et al., 2002; Zucker and Regehr, 2002). Although it is possible that CBs have some effect on regulating the availability of this specific group of ready-to-use SVs this remains to be established.

Physical signs of acute CB-intoxication include muscle weakness, difficulty of breathing and speech impairment (Castaneto et al., 2014). In particular, the hypoglossal motor nucleus (HN) sends rhythmic signals to the tongue muscles during breathing, chewing, swallowing and phonation. Abnormal activity of the genioglossus muscle of the tongue, innervated by hypoglossal motoneurons (HMNs), is central to obstructive sleep apnea in humans, which affects ~4% of adults (Horner, 2007). In this way, the hypoglossal motor system offers several advantages as an experimental model to study the feasible influence of CBs in the control of excitatory inputs incoming to motoneurons. First, motoneurons are arranged in the HN, which is located in the dorsal medulla and easily accessible for functional studies in animal models. Second, AMPA receptor (AMPAR)-mediated neurotransmission incoming to HMNs can be easily isolated *in vitro* and have been well characterized (Gonzalez-Forero et al., 2012). Third, from an experimental point of view, a considerable advantage of this motor system is that the inspiratory-related afferent activity in HMNs, almost exclusively mediated by AMPAergic signaling, persists even in the *in vivo* decerebrated preparation (Gonzalez-Forero et al., 2004; Rekling and Feldman, 1998). Therefore, the hypoglossal system is a useful model to scrutinize molecular and cellular mechanisms involved in the modulation of excitatory synaptic neurotransmission on motoneurons.

Here, we show that presynaptic CB1-mediated signaling induced rapid and reversible short-term depression (STD) of glutamatergic synapses on HMNs by, at least, reducing the size of the RRP of SVs. Remarkably, a CB agonist depressed inspiratory-related HMN activity *in vivo*, presumably via CB1. Data suggest that CBs can affect normal performance of motor output commands by directly modulating excitatory inputs on motoneurons.

2. Materials and methods

Wistar rats of either sex were obtained from an authorized supplier (Animal Supply Services, University of Cádiz, Spain), and were cared for and handled in accordance with the guidelines of the European Union Council (86/609/UE) and Spanish regulations (BOE 67/8509-12; BOE 1201/2005) and U.K. Animals (Scientific Procedures) Act, 1986 and associated guidelines on the use of laboratory animals. All efforts were made to minimize animal suffering, to reduce the number of animals used, and to utilize alternatives to *in vivo* techniques when available. Experimental procedures were approved by the local Animal Care and Ethics Committee. Adult animals were individually housed in cages with water and food pellets available *ad libitum*, under temperature controlled conditions at 21 ± 1 °C, with a cycle of 12 h light and 12 h darkness. Surgical procedures were carried out under aseptic conditions and after ensuring a sufficient depth of anesthesia evaluated by testing for the absence of withdrawal reflexes.

2.1. Extraction of brainstem slices

Brainstem slices were quickly obtained from rat pups (P6–P9) decapitated under anesthesia by hypothermia (placed on ice for 10–15 min) as previously described (Gonzalez-Forero et al., 2012). Briefly, dissection was in ice-cold (~4 °C) sucrose artificial CSF (S-aCSF) bubbled with 95% O_2 and 5% CO_2. S-aCSF composition was as follows (in mM): 26 $NaHCO_3$, 10 glucose, 3 KCl, 1.25 NaH_2PO_4, 2 $MgCl_2$, and 218 sucrose. Transverse slices (300–400 μm-thick) obtained using a vibroslicer (NVSL; WPI) were transferred to normal oxygenated aCSF (in mM: 26 $NaHCO_3$, 10 glucose, 3 KCl, 1.25 NaH_2PO_4, 2 $MgCl_2$, 130 NaCl, and 2 $CaCl_2$) and allowed to stabilize at ~37 °C for 30 min. Next, slices were either transferred to a recording chamber for whole-cell patch-clamp recordings or incubated for 10 min (~22 °C), with aCSF alone or supplemented with various drug treatments, before processing for electron microscopy.

2.2. Electron microscopy

Brainstem slices were fixed by 45-min immersion in 3.5% glutaraldehyde in 0.1 M phosphate buffer (PB), pH 7.4, at 36 °C (Gonzalez-Forero et al., 2012). The slices were rinsed and stored in PB with 0.05% sodium azide at 4 °C until electron microscopy processing. Sections were postfixed with 2% osmium tetroxide in PB for 90 min. Subsequently, the slices were dehydrated in graded series of ethanol and stained in 2% uranyl acetate in 70% ethanol at 4 °C. Afterward, sections were dehydrated again in graded series of ethanol, washed with propylene oxide, and embedded in Araldite resin. Ultrathin sections (70–80 nm-thick) obtained with an ultramicrotome (LeicaEMUC6) were analyzed under a FEI Tecnai Spirit electron microscope attached to a digital camera (Morada Preview). Images were analyzed using the ImageJ free software.

2.3. Whole-cell patch-clamp recordings

Whole-cell patch-clamp recordings were performed on HMNs from transverse brainstem slices (P6–P9 rat pups) as previously described (Gonzalez-Forero et al., 2012). Recordings were performed at 31 °C on slices superfused (rate ~3–4 ml/min) with aCSF solution equilibrated with 95% O_2 and 5% CO_2. Patch electrodes (1.5–3 MΩ resistance) contained a KGluconate-based internal solution (in mM: 17.5 KCl; 122.5 KGluconate, 9 NaCl; 1 $MgCl_2$; 10 HEPES; 0.2 EGTA; 3 Mg-ATP, 0.3 GTP-Tris, pH 7.2). Voltage-clamp recordings were obtained and low-pass bessel-filtered at 10 kHz with a MultiClamp 700B amplifier. Data were digitized at 20 kHz with a Digidata 1332A analog-to-digital converter, acquired and analyzed off-line using pCLAMP 9.2 software (Axon Instruments, Foster City, CA). Only recordings with access resistance between 5 and 20 MΩ were analyzed. The access resistance was checked throughout the experiments, and recording was abandoned if it changed >15%. Series resistance was regularly compensated by 65%–75%. Leak currents and liquid junction potentials were not corrected.

Whole-cell voltage-clamp recordings were used to analyze the effects of CB-mediated signaling modulators on synaptic strength at excitatory synapses on HMNs. To distinguish presynaptic effects of CBs, we performed an electrophysiological analysis of excitatory postsynaptic AMPA currents (EPSCs) evoked by electrical stimulation of afferent axons, synaptic facilitation of EPSCs following paired-pulse stimulation, AMPAergic miniature EPSCs (mEPSCs), spontaneous AMPA synaptic currents recorded under conditions of facilitated synaptic release (sEPSCs), and EPSCs evoked by a minimal stimulation paradigm. Whole-cell AMPAergic responses were recorded at a holding potential of −65 mV. EPSCs were pharmacologically isolated in the presence of 1 μM strychnine hydrochloride, 10 μM bicuculline methochloride, 30 μM D-tubocurarine, and 50 μM (DL)-APV applied to the bath perfusion (Fig. 1A). All these drugs were purchased from Tocris Cookson (Bristol, UK).

EPSCs were elicited by means of a concentric bipolar tungsten electrode placed in the ventrolateral reticular formation (VLRF) approximately 0.5–1 mm from the border of the HN. For paired pulse facilitation, VLRF was stimulated with pairs of electrical stimuli with inter-pulse intervals of 25 ms given with 30 s delay between pairs. Stimulation parameters (<400 μA, 50-μs pulse duration, delivered at 0.05 Hz) were chosen to generate a sizable and reproducible postsynaptic response. The stimulus intensity was adjusted to evoke a first EPSC of approximately 50% of maximal amplitude, which was then maintained constant throughout the recording period. A minimum of 10 responses was recorded under each pharmacological condition and averaged for the analysis of EPSC amplitude. Paired-pulse facilitation ratio (PPR) was computed by dividing the peak amplitude of the second response by the peak amplitude of the first one. In a group of experiments designed to investigate whether motoneurons are potential sources of eCBs, the depolarization-induced depression of excitation paradigm was carried out. After establishing a 25 s 0.2 Hz baseline, depolarization-induced depression of excitation was evoked by either, applying 5 depolarizing pulses (1 Hz) to the HMN with 100 ms duration to 0 mV, or by depolarizing the postsynaptic neuron to 0 mV for 60 s. Both depolarizing protocols were followed by resumption of a 0.2 Hz stimulus protocol.

The effect of CB modulators on EPSCs was also tested using a minimal-stimulation protocol. Pharmacologically isolated EPSCs were elicited by single pulses of minimum strength (0.2 Hz) delivered via the VLRF stimulation electrode. “Minimal” stimulation was defined as a percentage of EPSCs failures in the range

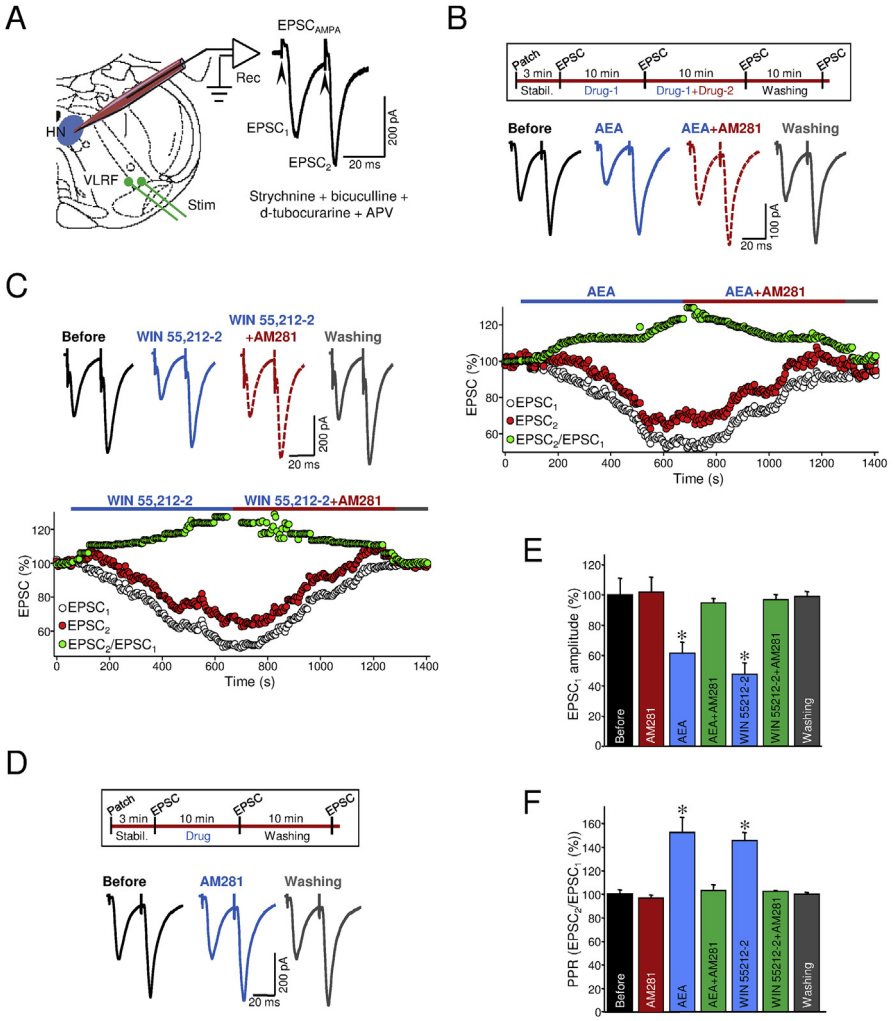

Fig. 1. AEA and WIN 55,212-2 rapidly and reversibly induce AMPAergic STD through presynaptic CB1 receptors. **A**, Schematic diagram of the *in vitro* experimental model used to analyze the effects of CB agonists on excitatory synaptic transmission to HMNs. Whole-cell patch-clamp recordings (Rec) were obtained from somata of HMNs in neonatal brainstem slices (P6–P9). AMPAergic excitatory postsynaptic currents ($EPSCs_{AMPA}$) were evoked by paired-pulse electrical stimulation (Stim) of the ventrolateral reticular formation (VLRF). The AMPAergic component was pharmacologically isolated in the presence of 1 μM strychnine hydrochloride, 30 μM D-tubocurarine, 50 μM (DL)-APV and, 10 μM bicuculline methochloride. **B**–**D,** Top, timing of experimental protocol. HMNs were initially allowed to stabilize (Stabil) with normal aCSF to obtain baseline control recordings. After that, slices were superfused for 10 min with aCSF supplemented with AEA (10 μM, B), WIN 55,212-2 (5 μM, C) or AM281 (0.5 μM, D) before current responses were measured. Slices were additionally incubated for 10 min with AEA plus AM281 (B) or with WIN 55,212-2 plus AM281 (C). Finally, a last round of acquisition was taken after a 10-min washout with drug-free aCSF. Middle, representative EPSCs recorded from HMNs at the indicated conditions in response to paired-pulse stimulation of VLRF. Bottom, representative time courses of the amplitude of the first (empty circles) and second (red circles) EPSC, and the $EPSC_2/EPSC_1$ ratio (green circles) in response to bath addition of indicated drugs. Data were normalized to values obtained at the "before" condition as 100%. **E**, **F**, Mean amplitude of the first EPSC and PPR ratio (25 ms inter-pulse intervals) under indicated treatments (before, n = 17 HMNs; AM281, n = 7 HMNs; AEA and AEA + AM281, n = 5 HMNs; WIN 55,212-2, n = 8 HMNs; WIN 55,212-2+AM281, n = 4 HMNs). The mean value for EPSCs recorded before drug perfusion was taken as 100% in each experimental group. PPR was obtained from the amplitude of the first and second EPSCs by the formula $EPSC_2/EPSC_1$. *$p < 0.05$, one-way ANOVA for repeated measures.

between 30% and 40%. The detection threshold was set at 3 times the root-mean-square noise (~9 pA). Evoked responses lower than the threshold level were counted as failures.

mEPSCs were pharmacologically isolated in the presence of 1 μM tetrodotoxin (TTX) and pharmacologically isolated with blockers of $GABA_A$, glycine, nicotinic and NMDA receptors applied to the bath perfusion. The recording of sEPSCs was performed under conditions of facilitated synaptic release without TTX in a modified extracellular solution containing high-Ca^{2+} (4 mM), high-K^+ (9 mM), and the receptor antagonists indicated above. The AMPAergic nature of both types of events (mEPSCs and sEPSCs) was previously reported (Gonzalez-Forero et al., 2012). For each cell and treatment condition, we obtained segments of continuous recording (5–8 min) of spontaneous activity. During analysis, the threshold level for detection of events was set as above. Spurious events and noise artifacts were manually rejected after visual inspection of the automatically screened events. For each cell, peak amplitudes and inter-event intervals of single mEPSCs and sEPSCs were measured across the different recording epochs and used to calculate mean values and generate cumulative probability plots.

In general, HMNs were initially perfused with normal aCSF to obtain baseline control data, followed by superfusion for 10 min with aCSF containing a given drug. In some experiments, a second drug was subsequently added to the perfusate and its effects tested 10 min later. Finally, a last round of acquisition was taken after a 10-min washout with drug-free aCSF.

2.4. In vivo microiontophoretic application of O-2545

Adult animals (250–350 gr) were prepared for extracellular recordings as reported previously (Montero et al., 2008). Briefly, rats were anesthetized (1.5–3% isoflurane mixed with 100% O_2) and injected i.m. with atropine (0.2 mg/kg) and dexamethasone sodium phosphate (0.8 mg/kg). A ventral approach was used to cannulate trachea, bladder, and femoral vein. Teflon-isolated silver bipolar electrodes were fixed around the right XIIth nerves. Subsequently, tracheotomized animals were vagotomized, decerebrated, paralyzed with gallamine triethiodide (20 mg/kg, i.v., initially; 4 mg/kg, i.v., as needed), and mechanically ventilated. Expired CO_2 and O_2 were monitored continuously and the end-tidal CO_2 was kept at 4.8%–5.2%. Rectal temperature was kept steady at 37 ± 1 °C.

Three-barreled glass pipettes, pulled and broken to a diameter of 5–7 μm, were used for single-unit recording and iontophoresis. The recording barrel (1–3 MΩ) was filled with 3 M NaCl. A second barrel was filled with O-2545 in distilled water.

Individual neuronal current response curves to O-2545 were determined by administering increasing currents (+20 to +140 nA, 20 nA steps, 30 s duration) through the drug barrel using the Neurophore BH-2 system (Harvard Apparatus). In a group of animals, systemic intravenous (iv.) administration of the CB1 antagonist AM281 (0.5 mg/kg) was performed 5 min before microiontophoretic application of O-2545. In order to exclude direct effects of current, pH and/or vehicle, 7 motoneurons were first tested by passing a current of 80 nA for 120 s containing vehicle (distilled water) and compared with subsequent application of a current with the same characteristics throughout the O-2545-containing solution.

HMNs were identified by their antidromic activation from the XIIth nerve and by the collision test (Montero et al., 2008). The electrical signals were amplified and filtered at a bandwidth of 10 Hz–10 kHz for display and digitization purposes. Only inspiratory HMNs discharging at basal conditions (end tidal CO_2 = 4.8–5.2%) were considered in this study. Unitary discharge activity was amplified, filtered, digitized and stored using the PowerLab/8SP A/D computer interface (ADInstruments, Castle Hill, Australia) for off-line analysis. The unitary mean firing rate (mFR) (spikes/s) in each burst was measured.

2.5. Drugs

AM281 (0.5 μM or 0.5 mg/kg, i.v.), Anandamide (AEA, 10 μM), O-2545 hydrochloride (20–25 mM), and WIN 55,212-2 (5 μM) were obtained from Tocris, UK.

2.6. Statistics

Data were obtained from at least 3 animals per experimental condition and are expressed as the mean ± standard error of the mean (SEM). Applied statistical tests per experimental condition are indicated in figure legends or in results. In all cases, the minimum significance level was set at $p < 0.05$.

3. Results

3.1. Presynaptic CB-triggered signaling mediates rapid and reversible STD at AMPAergic inputs on HMNs

In vivo, most HMNs exhibit a repetitive rhythmic firing consisting of inspiratory-related bursting discharges driven by excitatory brainstem afferences (Gonzalez-Forero et al., 2004; Peever et al., 2002). The inspiratory synaptic drive to HMNs is mediated by the excitatory amino acid glutamate mainly acting on AMPARs (Rekling and Feldman, 1998). Hence, we first scrutinized the functional effects of the eCB AEA (10 μM), which has higher affinity for CB1 than for CB2, and the synthetic CB WIN 55,212-2 (5 μM), a potent CB1 and CB2 agonist (Thakur et al., 2005), on EPSC by whole-cell patch-clamp recordings of HMNs (slices from P6–P9 rats). As we have recently reported (Gonzalez-Forero et al., 2012; Sunico et al., 2010), electrical stimulation of the VLRF evokes monosynaptic EPSCs in HMNs *in vitro* (Fig. 1A). In the voltage-clamp mode, application of the same type of stimulus consistently evoked large, inwardly directed, postsynaptic currents in HMNs held at −65 mV using KGluconate-filled electrodes. This response was almost fully suppressed with antagonists for AMPA (NBQX) and NMDA (APV) receptors (Gonzalez-Forero et al., 2012; Sunico et al., 2010). In the present study, we pharmacologically isolated the AMPAergic component of excitatory EPSCs by addition to the bath perfusion of strychnine, bicuculline, D-tubocurarine, and APV (Fig. 1A). Adding both CB agonists for 10 min to the bath solution strongly attenuated EPSC amplitude (AEA: −38.3 ± 7.3%; WIN 55,212-2: −52.3 ± 7.5%) (Fig. 1B, C, E). CB-induced STD was rapidly and fully reversed, either by co-perfusion with the selective CB1-antagonist AM281 (Pertwee, 2010) (0.5 μM) (AEA + AM281: −5.2 ± 3.0%; WIN 55,212-2+AM281: −3.2 ± 3.5%) or upon washing (−0.9 ± 3.3%) (Fig. 1B, C, E).

The possible presynaptic site of action was first evaluated by analyzing EPSCs facilitation using the paired-pulse stimulation protocol (Fig. 1A). Under repetitive stimulation, a change in the amount of facilitation is considered to be attributable to a presynaptic change in the release probability (Zucker and Regehr, 2002). Paired-pulse facilitation is believed to result from the accumulation of residual Ca^{2+} within synaptic terminals, leading to increased transmitter release and an increased size of the second potential of the pair. In addition, synapses with a high release probability tend to produce large amplitude EPSCs following single-pulse afferent stimulation and exhibit little facilitation upon repetitive stimulation. Therefore, if the CB-induced synaptic attenuation involved a presynaptic mechanism of action, it would be associated with an increase in the magnitude of facilitation. Interestingly, facilitated PPR showed a marked and reversible increase at 25 ms intervals after application of either AEA (+52.4 ± 13.1%) or WIN 55,212-2 (+45.6 ± 6.9%) that returned to control-like values after co-addition of AM281 (AEA + AM281: +3.2 ± 4.8%; WIN 55,212-2+AM281: +2.4 ± 0.8%) (Fig. 1B, C, F). AM281 did not alter EPSCs amplitude (3.1 ± 9.5%) nor PPR (−3.8 ± 3.7%) *per se* (Fig. 1D–F). Thus, these outcomes indicate that baseline CB1-mediated signaling, if any, was not sufficient to modulate analyzed synaptic parameters, at least in our experimental conditions.

The preceding results show that the attenuation of the evoked AMPAergic responses induced by CB agonists was related to a reduced presynaptic probability of glutamate release and to an increase in the amount of facilitation. Mechanisms accounting for these alterations can involve changes in the excitability of presynaptic elements and/or in the probability of quantal release (Bellingham and Berger, 1996; Doze et al., 1991; Scanziani et al., 1992). These mechanisms can be discerned by comparing the effects of WIN 55,212-2 on miniature (quantal) EPSCs (mEPSCs) activity and on spontaneous EPSCs (sEPSCs) activity. Miniature quantal events represent the postsynaptic responses to transmitter release from single vesicles, and their average amplitude is usually taken as a measure of the sensitivity and/or number of postsynaptic receptors (Carroll et al., 1999; Turrigiano et al., 1998). Alterations in mEPSC amplitude and/or frequency can also serve as useful indicators of action potential-independent mechanisms that control synaptic transmission at pre- or postsynaptic locations. In this way, if WIN 55,212-2 acts to reduce presynaptic quantal release probability in an action potential-independent Ca^{2+} entry, mEPSC frequency should decrease; if WIN 55,212-2 acts to diminish postsynaptic glutamate receptor responses, a decrease in mEPSC amplitude should be expected. In the presence of TTX (1 μM) to block presynaptic action potentials, application of WIN 55,212-2 had no significant effect on the mEPSC amplitude (Fig. 2A, B). Thus, the mean amplitude of mEPSCs recorded after 10 min exposure to this drug was 20.8 ± 0.8 pA, which was similar to the average amplitude of mEPSCs measured before drug exposure (21.0 ± 0.8 pA; Fig. 2B). This was also supported by the drug's lack of effect on the distribution histogram (Fig. 2D) and cumulative probability functions (Fig. 2E; $p > 0.05$; Kolmogorov–Smirnov test) of mEPSC amplitude. WIN 55,212-2 induced, however, a subtle, but significant, reduction in the mEPSC frequency relative to the control condition (before: 5.8 ± 0.3 Hz; WIN 55,212-2: 5.1 ± 0.5 Hz; Fig. 2C). These results suggest that the CB agonist acts to decrease action potential-independent quantal release probability, and also support that WIN 55,212-2 does not alter postsynaptic glutamate receptor response.

In light of these results, we considered the possibility that depression of excitatory synaptic responses by WIN 55,212-2 was due to a presynaptic mechanism. To further explore this mechanism we recorded spontaneous AMPAergic synaptic currents under conditions of facilitated spontaneous glutamate release (sEPSCs). Under these pharmacological conditions, spontaneous synaptic activity consist of a mixture of presynaptic activity (action potential)-dependent transmitter release and random activity-independent transmitter release. Under control pretreatment conditions sEPSCs had a mean amplitude of 91.9 ± 10.7 pA, and a mean frequency of 8.6 ± 0.7 Hz; after WIN 55,212-2 treatment, the mean sEPSC amplitude and frequency were significantly reduced to 30.8% (28.4 ± 2.6 pA) and to 66.1% (5.7 ± 0.9 Hz), respectively

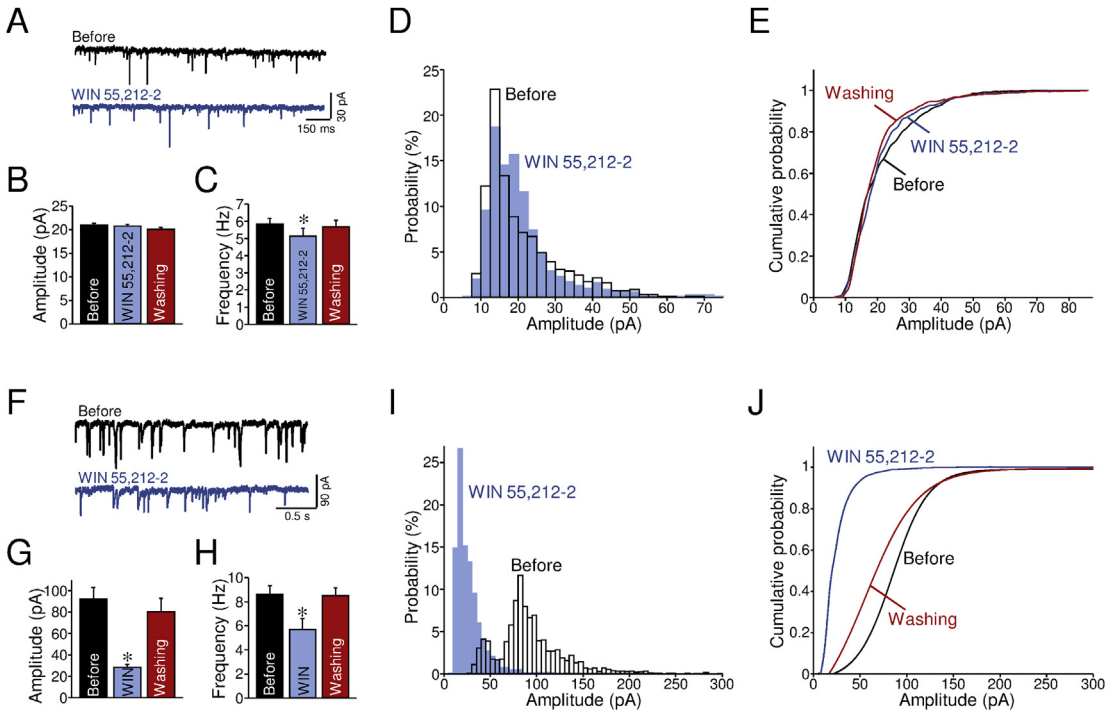

Fig. 2. WIN 55,212-2 affects mEPSCs and sEPSCs. **A**, Traces of spontaneously occurring mEPSCs recorded from a representative HMN before and after 10 min bath perfusion with WIN 55,212-2. The cell was held at −65 mV during recording. Quantal AMPAergic currents (mEPSCs) were isolated with TTX (1 μM), bicuculline (10 μM), strychnine (1 μM), APV (50 μM), and D-tubocurarine (30 μM). **B**, **C**, Average mEPSC amplitude (B) and frequency (C) for the WIN 55,212-2-treated group of HMNs compared with their respective pre-treatment (before) and washout periods. **D,** Amplitude distribution histograms of mEPSCs before and during WIN 55,212-2 treatment. Each histogram is made of 680 events (5 pA bin size). **E**, Cumulative probability functions of mEPSCs amplitude recorded before (black line), during WIN 55,212-2 treatment (blue line), and after washout (red line). Bin width: 2 pA. Data were pooled from 4 HMNs. **F**, **G**, **H**, **I** and **J** as in A, B, C, D and E, respectively, but for spontaneous EPSCs (sEPSCs). sEPSCs were isolated in the presence of bicuculline, strychnine, APV, and D-tubocurarine and recorded at −65 mV in a high-K^+, high-Ca^{2+} containing aCSF without TTX. Each histogram is made of more than 1800 events and data were pooled from 4 HMNs. $^*p < 0.05$, one-way ANOVA for repeated measures. (For interpretation of the references to colour in this figure legend, the reader is referred to the web version of this article.)

(Fig. 2F–H). Consequently, the distribution histogram (Fig. 2I) and the cumulative probability function (Fig. 2J) of sEPSC amplitude were significantly shifted to the left, indicating lower event amplitudes after treatment ($p < 0.001$; Kolmogorov–Smirnov test). sEPSC amplitude and frequency recovered after washout (Fig. 2F–J). These results are more consistent with the idea that WIN 55,212-2 also elicits depression of action potential- and Ca^{2+}-dependent glutamatergic transmission through presynaptic modifications involving reduction in the probability of quantal and activity-dependent transmitter release.

Release probability at single central synapses is believed to be determined by the number of fusion-competent vesicles (Dobrunz, 2002; Millar et al., 2002). Therefore, changes in synaptic strength induced by CB agonists could reflect a decrease in the size of the RRP of SVs. This idea was further strengthened by the subsequent analysis of EPSC amplitude using a minimal stimulation paradigm, which is designed to stimulate only one fiber and a single or small number of release sites. Characteristically, the intensity of the stimulation was set to elicit EPSCs with 30%–40% failures (Fig. 3A, B) (Gonzalez-Forero et al., 2012). Under the control condition EPSC amplitudes evoked by minimal stimulation were distributed over a range from zero to around 115 pA (Fig. 3A, C), with a mean amplitude of 29.8 ± 3.3 pA (excluding failures). WIN 55,212-2 reversibly enhanced the failure probability (before: 36.3 ± 1.1%; WIN 55,212-2: 78.6 ± 2.8%) and reduced EPSC amplitude (18.9 ± 2.0 pA, excluding failures), narrowing the amplitude distribution toward lower amplitudes (≤35 pA) under the minimal stimulation protocol (Fig. 3A–C). Thus, the cumulative distribution of EPSC amplitude was displaced to the left after WIN 55,212-2 treatment ($p < 0.001$; Kolmogorov–Smirnov test) (Fig. 3D).

Together, these data strongly suggest that the depression of synaptic strength induced by CB agonists is completely dependent on a reduction in the release probability from excitatory glutamatergic terminals apposed on HMNs, an effect probably attributable to a reduction in the RRP of SVs. These outcomes support that CB agonists induce AMPAergic STD by acting mainly via presynaptic CB1.

3.2. *WIN 55,212-2 reduces the size of the RRP of SVs in excitatory boutons*

At this point, we hypothesized that WIN 55,212-2-induced STD is underpinned by reordering of the clustering and spatial distribution of SVs within excitatory boutons. Therefore, we analyzed the ultrastructural organization of S-type synaptic boutons, which are presumably excitatory (Bodian, 1966; Gray, 1959; Uchizono, 1965), attached to HMNs in control and treated neonatal brainstem slices by electron microscopy. Under electron microscopy, HMNs are easily distinguishable from interneurons, which present a noticeable invaginated nucleus and smaller soma sizes in cross-sectional areas at the nucleolar level (Sunico et al., 2011). S-type boutons were classified by the type of SVs (spherical), assisted by asymmetric synaptic densities when these were evident (Sunico et al., 2011, 2010). To quantify the spatial distribution of SVs relative to the active zone (a.z.) within S-type boutons, three regions were delimited by lines parallel to the a.z. profile and we counted the number of vesicles included in the intervals of 0–100 nm, 100–200 nm, and 200–300 nm from the a.z. To evaluate feasible effects on vesicle trafficking and/or recycling, we also counted the number of SVs included in

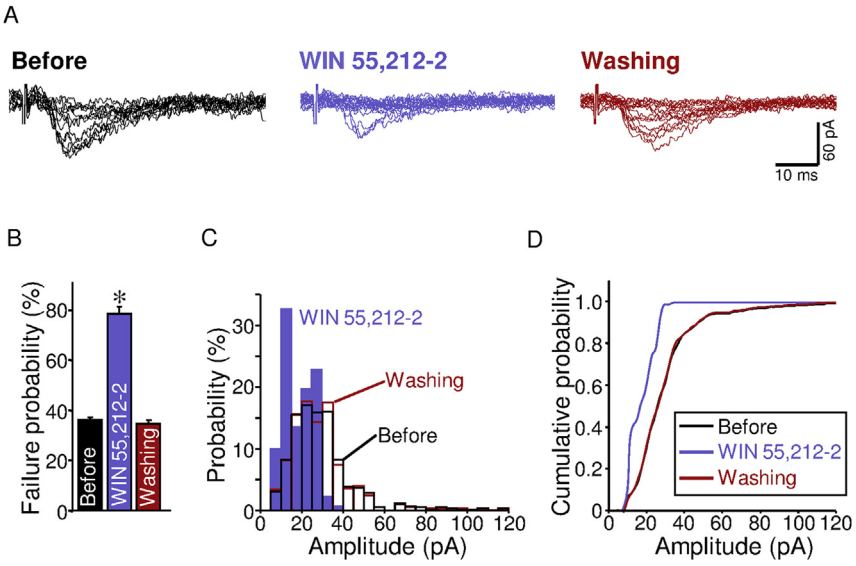

Fig. 3. WIN 55,212-2 increases failure probability to evoke EPSCs by minimal stimulation. **A**, Superimposition of 15 successive EPSCs evoked at 0.2 Hz by minimal stimulation of VLRF in HMN before, following WIN 55,212-2 (10 μM) perfusion, and after washout. **B**, Histogram showing changes in EPSC failure rates to minimal stimulation for the control, WIN 55,212-2, and washout conditions (n = 4 HMNs). *$p < 0.05$, one-way ANOVA for repeated measures. **C,** Amplitude distribution histograms of EPSCs. Each histogram is made of 600 responses (5 pA bin size). **D**, Normalized cumulative probability distributions of EPSC amplitude. Bin width: 2 pA. Plots in C and D were constructed excluding failures (n = 4 HMNs).

the total pool for each analyzed bouton in the same section where intervals were analyzed (Gonzalez-Forero et al., 2012). Accordingly, excitatory, spherical SV-containing boutons (S-type), attached to HMNs from WIN 55,212-2-treated (5 μM) slices, evidenced a prominent reduction in the number of SVs near the a.z. (Fig. 4A, B, D). The region closest to the a.z. showed a decline in the number of SVs after WIN 55,212-2 treatment (0–100 nm: −17.0 ± 5.5%), along with a non-significant reduction in the more distant regions (Fig. 4D). Non-significant changes were observed in AM281-incubated (0.5 μM) slices (Fig. 4C, D). Since WIN 55,212-2-treatment did not alter the size of the total SV pool, effects on SV trafficking and/or recycling are unlikely (Fig. 4D). No effects were observed on the average a.z. length, mean number of a.z. per bouton, average number of excitatory boutons per motoneuron, and mean cross-sectional bouton area (Table 1). Altogether, these observations indicate that the attenuation of glutamatergic transmission induced by WIN 55,212-2 is the consequence, at least in part, of a redistribution of the SV pool within excitatory terminals rather than a disruption of SV trafficking and/or recycling.

Given that WIN 55,212-2 induced a change in the distribution of excitatory SVs, we next performed ultrastructural studies to investigate whether the CB agonist modifies the size of the RRP of SVs. Since it has been proposed that morphologically docked SVs correspond to the release-ready neurotransmitter quanta (Schikorski and Stevens, 2001), we measured the linear density (number of SVs/μm of membrane) of docked SVs at the a.z. WIN 55,212-2, but not AM281, led to a reduction (−65.2 ± 6.0%) in the number of docked SVs (control: 5.7 ± 0.4 SVs/μm; WIN 55,212-2: 2.0 ± 0.3 SVs/μm) (Fig. 4E, F). These outcomes strongly support that the CB agonist may regulate the size of the RRP of SVs in S-type boutons.

In summary, these data indicate that the attenuation of glutamatergic transmission on HMNs induced by CB agonism is the consequence, at least in part, of a redistribution of the vesicle pool within the terminal which directly affects the RRP of SVs rather than a disruption of vesicle trafficking and/or recycling.

3.3. AM281 prevents depolarization-induced depression of EPSC

eCBs are thought to be released from depolarized postsynaptic neurons in a Ca^{2+}-dependent manner and act retrogradely on presynaptic CB1 receptors to suppress inhibitory or excitatory neurotransmitter release. Depolarization-induced depression of excitation appears to be an important form of short-term neuronal plasticity involving eCB as retrograde messengers and the activation of presynaptic CB1 receptors to reduce glutamate release. This eCB-mediated modulation of excitatory synapses has been described in the hippocampus and cerebellum (Kreitzer and Regehr, 2001; Maejima et al., 2001; Ohno-Shosaku et al., 2002), but evidence on depolarization-induced CB1-dependent synaptic plasticity in a motor nucleus is lacking. Therefore, we explored whether this plastic event modulates excitatory inputs arriving to HMNs and we subsequently studies the possible contribution of CB1. EPSCs evoked in HMNs in response to stimulation of VLRF (0.2 Hz) were recorded before and after application of two depolarization protocols. First, after a stable synaptic response was confirmed for 25 s, we found that depolarization of HMNs (5 depolarizing pulses (1 Hz) with 100 ms duration to 0 mV) induced transient depression (−19.4 ± 0.4%) of EPSCs together with an increase (+24.9 ± 1.5%) in the PPR (Fig. 5A, B). Both parameters recovered to baseline condition 35–45 s after depolarization. Second, stepping the voltage of the postsynaptic HMN from −65 mV to 0 mV for 60 s resulted in a more accentuated depression (−54.6 ± 4.7%) of EPSCs immediately after depolarization lasting 130–160 s (Fig. 5C, D). However, long-lasting depolarization was accompanied by a change (+23.6 ± 1.5%) in the PPR similar to those induced after the brief depolarizing protocol (Fig. 5B, D). Depolarization-induced depression of EPSCs and PPR alterations were fully abolished by pretreatment for 10 min with the CB1 antagonist AM281 (Fig. 5B, D). These results support that depolarization of HMNs produces retrograde signals that act on CB1 receptors on excitatory inputs. These outcomes point to motoneurons as another neuronal type that might produce eCBs

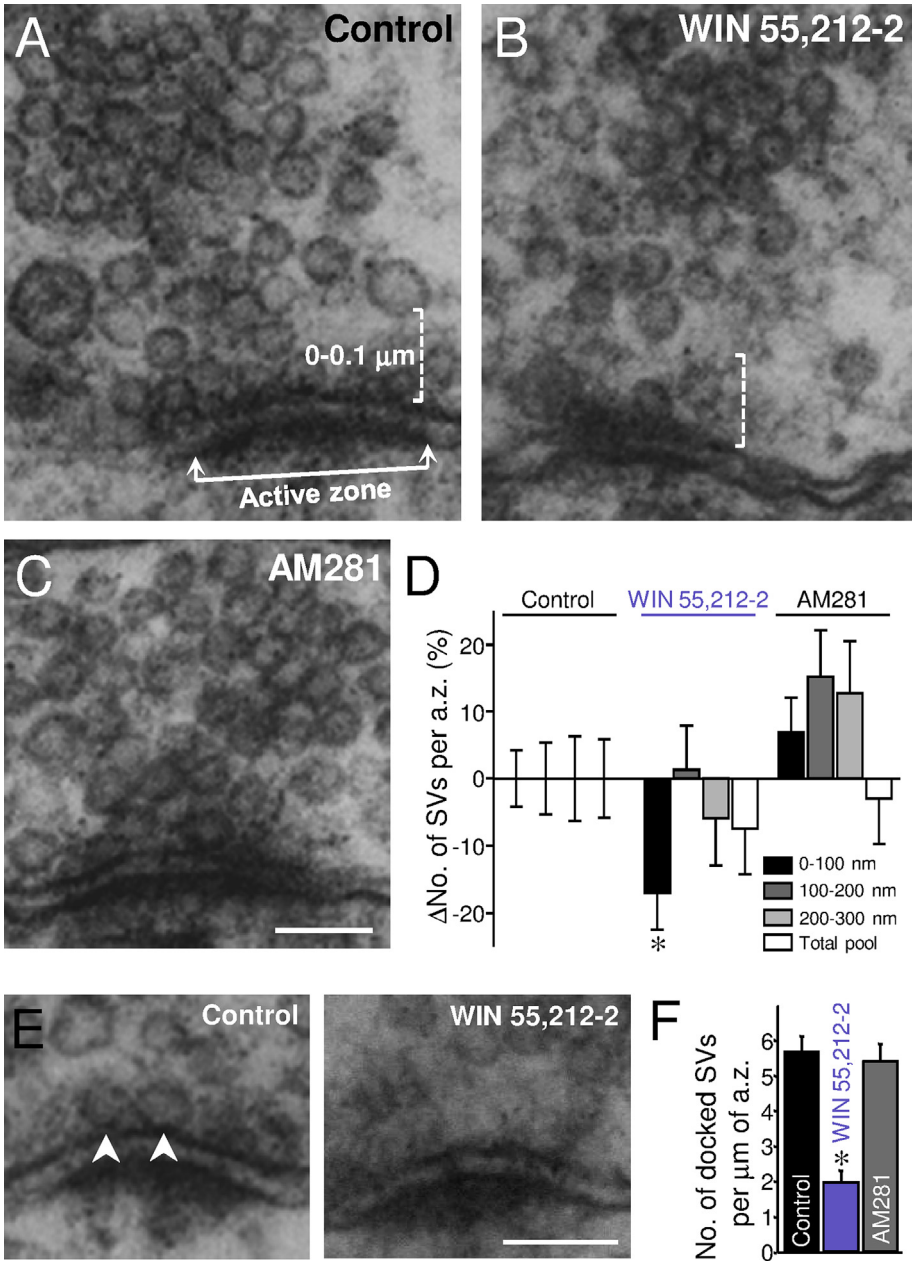

Fig. 4. WIN 55,212-2 leads to spatial distribution reordering of SVs in S-type boutons. **A–C**, Electron micrographs of spherical-containing vesicles, S-type boutons with asymmetric synaptic contacts on the somatic membrane of HMNs from rat pups following incubation of brainstem slices in aCSF alone (control) or supplemented with WIN 55,212-2 (10 μM) or AM281 (0.5 μM). The boxed region (white dotted line) encloses the area directly adjacent to the a.z. membrane. Scale bar, 100 nm. **D**, Changes in the number of SVs (percentage change from control) contained in each spatial compartment (control, n = 105 boutons; WIN 55,212-2, n = 76 boutons; AM281, n = 87 boutons). Histogram bins indicate distances from the a.z. as indicated in the legend. **E**, High-magnification electron microscopy images showing in detail SVs docked to asymmetric a.z. (arrowheads). In this example, no docked SV is observed under WIN 55,212-2 treatment. Scale bar, 100 nm. **F**, Histogram showing the linear density of docked synaptic vesicles per micrometer of a.z. under the indicated conditions. $^{*}p < 0.05$, one-way ANOVA, *post hoc* Tukey test.

which, as retrograde messengers, can modulate incoming excitatory synaptic drive acting via presynaptic CB1 receptors.

3.4. O-2545 depresses baseline inspiratory-related activity of adult HMNs in vivo

Since CB agonists strongly reduce excitatory synaptic strength on HMNs *in vitro*, we finally investigated whether CB-triggered signaling has any relevant action on motor output command performance in adulthood. In decerebrated animals, HMNs exhibit rhythmic inspiratory-related bursting discharges (Fig. 6A) driven by glutamatergic brainstem afferents, mainly acting on AMPARs, with little or no contribution of inhibitory inputs (Gonzalez-Forero et al., 2004; Peever et al., 2002). Unitary extracellular recordings were performed from antidromically identified HMNs subjected to microiontophoretic ejection of the water-soluble synthetic high affinity CB agonist O-2545 (25 mM; for 30 or 120 s). Administration of the synthetic CB for 30 s produced a current-dependent decrease in the inspiratory-related discharge activity (mFR/burst) of motoneurons (Fig. 6B–D). Data were well fitted to sigmoid equations ($p < 0.0001$, $r^2 > 0.98$), reaching maximal alterations of mFR/burst at the highest current injection tested +140 nA (−25.5 ± 4.2%)

Table 1
Ultrastructural characterization of S-type boutons attached to HMNs.

	Length of a.z. (μm)	No. of a.z. per bouton	Bouton area (μm^2)	No. of boutons/HMN
Control	0.25 ± 0.08 (124)	1.21 ± 0.04 (105)	0.50 ± 0.02 (102)	2.1 ± 0.2 (80)
WIN 55, 212-2	0.24 ± 0.09 (93)	1.25 ± 0.06 (76)	0.46 ± 0.03 (75)	2.6 ± 0.3 (60)
AM281	0.26 ± 0.09 (103)	1.22 ± 0.05 (87)	0.54 ± 0.03 (85)	2.0 ± 0.2 (85)

Number of sampled boutons or active zones (a.z.) is indicated in parentheses.

(Fig. 6B–D). Interestingly, previous intravenous administration of AM281 fully avoided the effects of current application (+120 nA) through a pipette barrel containing the CB agonist O-2545 (Fig. 6D). AM281 was injected at least 5 min before microiontophoretic application of O-2545. However, systemic administration of the CB1 antagonist AM281 alone had no significant effects on mFR/burst (32.4 ± 2.0 spikes/s; n = 30 HMNs) relative to the control untreated condition (35.7 ± 2.1 spikes/s; n = 47 HMNs). In addition, 7 motoneurons tested for O-2545 were subjected to a constant ejection current for 2 min. Each HMN was tested first for vehicle (distilled water) and then for O-2545 administration (Fig. 6E). CB agonist administration (25 mM; 80 nA) induced a significant decrease in the firing rate of HMNs (Fig. 6E) of −10.6 ± 5.3% in relation to the vehicle condition ($p < 0.05$, one-way ANOVA for repeated measures). Altogether, these data strongly support that CB1-triggered signaling plays a major role in affecting motor output performance by restraining baseline inspiratory-related activity of the motoneuron pool in adulthood. Furthermore, these outcomes are in agreement with a CB1-induced attenuation of glutamatergic synaptic influence incoming on HMNs *in vivo*.

4. Discussion

We show here that the eCB AEA and the synthetic CB agonist WIN 55,212-2 induce rapid and reversible STD at glutamatergic synapses on HMNs mainly through presynaptic CB1. The mechanism of action involves, at least, reducing the RRP of SVs at excitatory boutons in contact with motoneurons. Additionally, motoneurons are potential sources of eCBs that act as retrograde messengers regulating incoming synaptic information via presynaptic CB1. Finally, local application of a CB agonist depresses the inspiratory-related discharge activity of HMNs presumably in a CB1-dependent way. This provides a feasible basis for muscle weakness and motor performance impairment associated with cannabis consumption. Furthermore, these results highlight a feasible mechanism by which CBs, as anti-excitotoxic agents, might have neuroprotective properties and, as antispastic drugs, relieve motor symptoms in multiple sclerosis (MS) patients.

Two main CB receptors (CB1 and CB2) are part of the eCB signaling system. CB1s are widely expressed in the brain and mediate inhibition of neurotransmitter release from presynaptic terminals, while CB2s are typically found in the immune system

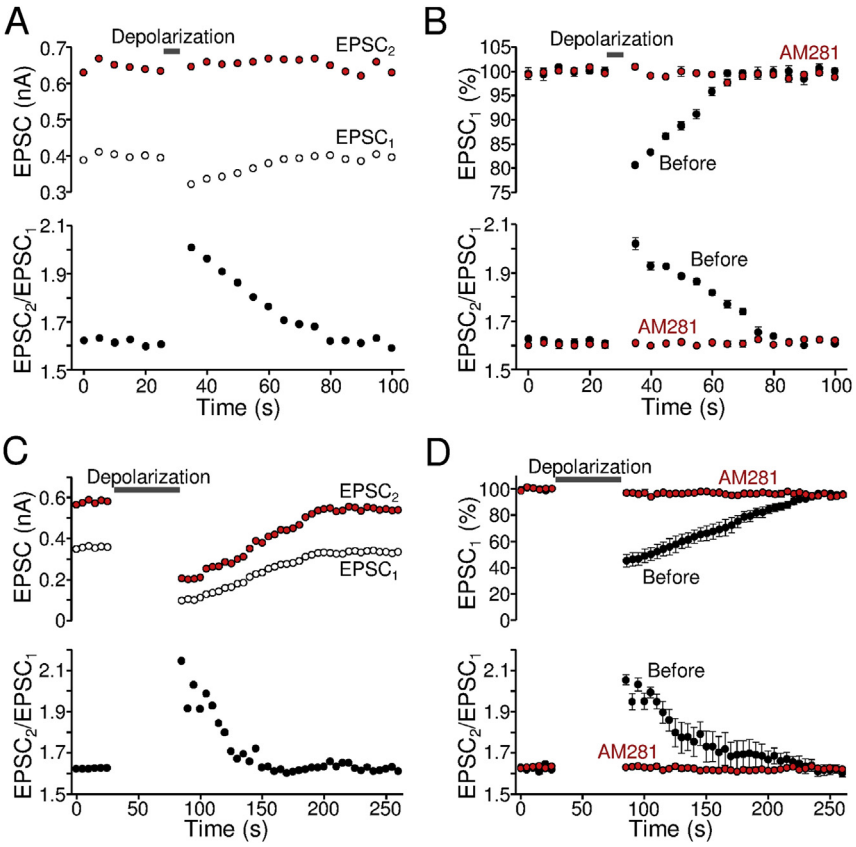

Fig. 5. AM281 abolishes depolarization-induced depression of EPSCs. A, Time course of the $EPSC_1$ (open circles) and $EPSC_2$ (red circles) amplitude (top) and PPR (bottom), recorded in a HMN before and after depolarizing stimulus (horizontal gray bar; 5 depolarizing pulses (1 Hz) with 100 ms duration to 0 mV). **B**, Time course of the averaged amplitude of $EPSC_1$ (top) and PPR (bottom) before and after depolarizing protocol in control condition (black circles) and after treatment for 10 min with the CB1 antagonist AM281 (red circles). Top, for normalization the mean value for $EPSCs_1$ amplitude obtained before depolarization in untreated neurons was taken as 100% (n = 5 HMNs). **C**, **D**, Same as in A, B, respectively, but stimulus consisted of depolarization of the postsynaptic neuron to 0 mV for 60 s (n = 5 HMNs). (For interpretation of the references to colour in this figure legend, the reader is referred to the web version of this article.)

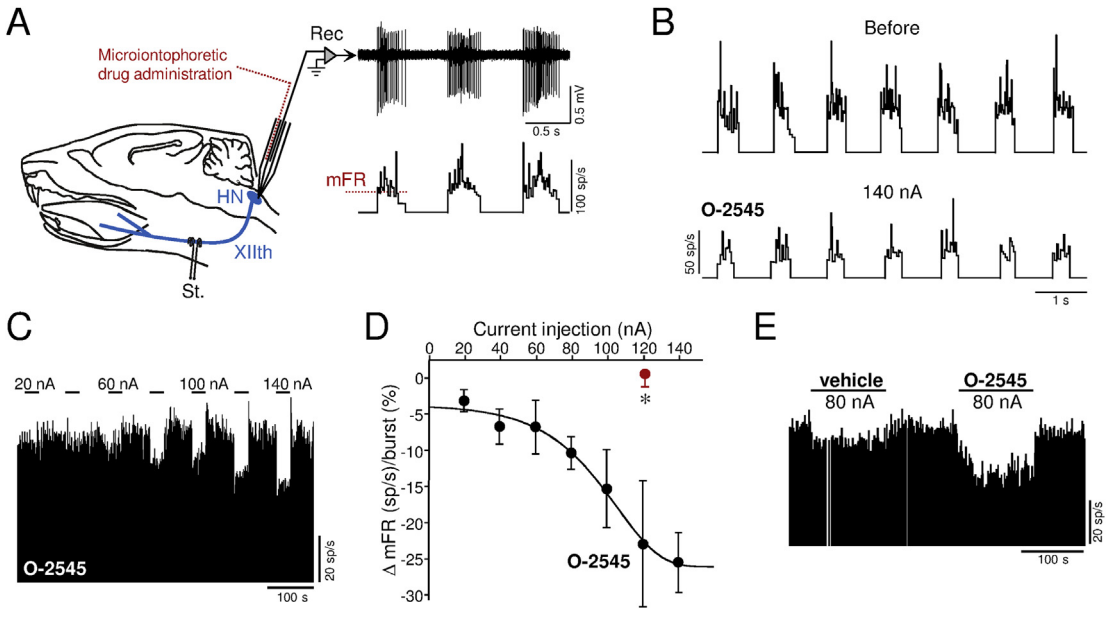

Fig. 6. O-2545 depresses inspiratory-related activity of HMNs. **A**, Schematic diagram of the *in vivo* experimental preparation. Unitary discharge activity (Rec) of HMNs was obtained in decerebrated, vagotomized and artificially ventilated adult rats, which had been injected with a neuromuscular blocking agent. A three-barreled pipette with a barrel for electrophysiological recordings and another for microiontophoretic administration of a drug is illustrated. Traces represent the extracellularly recorded spike discharge for an inspiratory HMN (top) and the histogram of the instantaneous firing rate (FR, in spikes/s; bottom). Mean firing rate (mFR, red dotted line) in each burst was measured and subsequently plotted along time. **B**, Instantaneous firing rates (sp/s) of a HMN in response to microiontophoretic administration of O-2545 (25 mM) at the indicated current. During the "before" condition a retention current of −5 nA is continuously applied. **C**, Time course of the mean firing rate (mFR, spikes/s) per burst in response to microiontophoretic administration (30 s on, 60 s off) of O-2545 at the indicated applied currents. **D,** Mean current–response curve illustrating the effects of O-2545 (n = 5 HMNs) on motoneuron activity characterized by the change in the mFR per burst. The effect of current application (+120 nA) through a barrel containing O-2545 in animals that previously received AM281 intravenously is also shown (red circle; n = 11 HMNs). $^{*}p < 0.05$, nonparametric Mann–Whitney *U* test. **E**, Illustrative response of a HMN to the microiontophoretic application (120 s on, 120 s off) of vehicle (distilled water) and successive ejection of O-2545 by application of the indicated current. (For interpretation of the references to colour in this figure legend,the reader is referred to the web version of this article.)

and are poorly expressed in the nervous system (Castillo et al., 2012; Kano et al., 2009). However, CB2s exert autocrine regulation of neuronal activity (den Boon et al., 2012). In our study, CBs-induced AMPAergic STD was fully reversed by the CB1-selective antagonist AM281. Nevertheless, these data appear to disagree with the facilitating effects of tetrahydrocannabinol on EPSPs in these motoneurons. The parallel rise in membrane resistance induced by tetrahydrocannabinol could mask actual presynaptic inhibitory effects on neurotransmitter release and synaptic current (Turkanis and Karler, 1983). Exogenous application of CBs increased the facilitation of PPR, which was reversed by the CB1 antagonist AM281. Under repeated stimulation, an increase in the amount of facilitation is considered to be attributable to a presynaptic decrease in the probability of vesicular transmitter release (Zucker, 1989; Zucker and Regehr, 2002). Therefore, the present results indicate that CB1-mediated signaling on excitatory presynaptic terminals causes the suppression of transmitter release, which is in agreement with previous reports (Kano et al., 2009). The presynaptic site of action for CBs gains further support since the synthetic CB agonist elicited a reduction in the event frequency of both miniature and spontaneous EPSCs, along with a decline in the amplitude of the spontaneous ones. Therefore, CBs can modulate glutamatergic transmission incoming to motoneurons through reduction in the probability of quantal and action potential- and Ca^{2+}-dependent transmitter release. These outcomes agree with previous results obtained from substantia gelatinosa neurons (Morisset and Urban, 2001), proopiomelanocortin neurons of the hypothalamic arcuate nucleus (Ho et al., 2007), supraoptic magnocellular neurons (Hirasawa et al., 2004), cultured hippocampal pyramidal neurons (Sullivan, 1999) and nucleus accumbens neurons (Robbe et al., 2001). Additionally, astrocytes could contribute to CB-induced AMPAergic STD. Astrocytic CB1s seem to be a $G_{q/11}$ protein-coupled receptor (Navarrete and Araque, 2008) and a $G_{q/11}$-selective inhibitor, YM-254890, did not prevent WIN 55,212-2-induced AMPAergic STD (García-Morales and Moreno-López; unpublished observations); therefore, astrocytes involvement is unlikely. These observations confirm that CBs may regulate glutamatergic synapses on HMNs via presynaptic CB1.

Most HMNs discharge inspiratory-related bursts of action potentials driven mainly by glutamatergic brainstem afferences, acting throughout AMPARs, with little or no contribution of inhibitory inputs (Gonzalez-Forero et al., 2004; Rekling and Feldman, 1998). Microiontophoretic application of the CB agonist O-2545 induced a reduction in the inspiratory-related activity of recorded HMNs an effect that was absent after previous systemic administration of the CB1-antagonist AM281. This agrees with a CB1-mediated depression of AMPAergic inputs rather than with a recruitment of silent inhibitory inputs. However, this last alternative should likely be discarded because eCBs depress glycinergic synaptic transmission on HMNs (Lozovaya et al., 2011; Mukhtarov et al., 2005). The present findings suggest that CBs may depress motoneuron activity by directly interfering with glutamatergic signaling via CB1 receptors. This could partially support the dysarthria, muscle weakness and difficulty breathing often manifested by cannabis users.

In vitro experiments shown that depolarization of postsynaptic HMNs induced a depression of excitation accompanied by clear increases in the PPR, both abolished by AM281. These outcomes indicate that depolarization-induced depression of excitation is expressed presynaptically as a decrease in excitatory transmitter release, and point to motoneurons as activity-dependent sources of eCBs, which in turn retrogradely act on presynaptic CB1 reducing the probability of vesicular transmitter release. eCB-mediated modulation of excitatory synapses has been also previously

reported to occur in other central structures, such as the hippocampus and cerebellum (Kreitzer and Regehr, 2001; Maejima et al., 2001; Ohno-Shosaku et al., 2002). However, our results *in vivo* after systemic administration of the CB1 antagonist did not contribute evidence related to the ongoing action of eCBs in the processing of baseline incoming inspiratory-related synaptic activity on HMNs, at least not in our experimental conditions. Whether the lack of any effect on inspiratory activity of HMNs results from the absence of eCB production by motoneurons or from compensatory effects of the systemic application of the CB1 inhibitor remains to be investigated. The finding that systemic administration of AM281 avoids inspiratory-related activity depression induced by microiontophoretic application of O-2545 excludes inadequate action by the antagonist and strongly supports that O-2545 effects are CB1-mediated. eCBs are synthesized "on demand" in stimulated neurons and released from them in a Ca^{2+}-dependent manner (Castillo et al., 2012; Kano et al., 2009). For retrograde eCB signaling, postsynaptic neuronal depolarization elevates intracellular Ca^{2+} via voltage-gated calcium channels and elicits eCBs production presumably by activating Ca^{2+}-sensitive enzymes (Castillo et al., 2012; Kano et al., 2009). Given that inspiratory-related activity of HMNs is mediated mainly by AMPA receptors (Gonzalez-Forero et al., 2004; Rekling and Feldman, 1998), which are permeable mainly to Na^{+} and K^{+}, it can be hypothesized that coupled synthesis of eCBs to inspiratory-related activity in HMNs could be scarce, or nonexistent, in our experimental conditions. Evidence of further Ca^{2+} entry downstream recruitment of another synaptic inputs and neurotransmitter receptors would induce eCB production by adult HMNs *in vivo* remains elusive.

Fine-tuning the size of the RRP of SVs is an essential determinant of synaptic strength, short-term plasticity, and inter-synaptic crosstalk (Gonzalez-Forero et al., 2012). Depletion of some ready-to-use pool of SVs generally lies behind diverse forms of STD (Schneggenburger et al., 2002; Zucker and Regehr, 2002). CB attenuation of the evoked AMPAergic current was related to a reduction in the glutamate release probability and to an increase in the amount of facilitation. Release probability at single central synapses is mainly determined by the number of fusion-competent SVs (Millar et al., 2002). This idea was further strengthened by the effects of WIN 55,212-2 on EPSCs amplitude using a minimal stimulation paradigm, which is designed to stimulate only one fiber and a single or small number of release sites. In addition, ultrastructural findings strongly support that functional synaptic changes are mainly explained by a depletion of the RRP of SVs. Actin filaments form an intricate cytoskeletal network that associates closely with SVs and a.z. Changes in the actin cytoskeleton are a prerequisite for exocytosis, enabling docking and fusion of SVs with the plasmalemma (Moreno-Lopez et al., 2011). In this context, inhibition of endogenous Rho kinase (ROCK), which regulates actin cytoskeletal rearrangements, reduces the RRP of SVs at excitatory inputs (Gonzalez-Forero et al., 2012). Strikingly, an AEA analog controls human breast cancer cell migration via ROCK inhibition (Laezza et al., 2008). Future research is needed to understand the mechanism by which presynaptic CB1 impairs SVs from docking to the a.z. and whether it involves reordering of actin filaments downstream from ROCK inhibition.

Glutamatergic-induced excitotoxicity is one of the most studied mechanisms mediating neuron degeneration in many neuropathological states. Therefore, CB-evoked reduction of glutamate release may underlie neuroprotective properties attributed to these lipid messengers by attenuating excitotoxic stimuli (Grundy et al., 2001; van der Stelt et al., 2002). CBs can alleviate tremor and spasticity in animal models of MS (Croxford, 2003). Strikingly, CBs have also manifested beneficial effects by relieving spasticity in patients with MS (Pertwee, 2007). Central network de-inhibition and/or over-excitation can result in motoneuron hyperactivity, which evokes the characteristic muscle hypertonia underlying spasticity. Therefore, CBs-induced attenuation of central excitatory signaling that leads to depression of motoneuron activity might mechanistically support the alleviation of motor over-activity in MS.

Author contributions

V.G.-M. and F.M.: collection, analysis and interpretation of data; B. M.-L.: conception and design of the experiments, interpretation of data and drafting the article. All authors approved the final version.

Funding

This work was supported by grants from Spain's Ministerio de Economía y Competitividad (SAF2011-23633) and the Junta de Andalucía's Consejería de Innovación, Ciencia y Empresa (PAI2011-CTS-7281) to B.M.-L. PAI2011-CTS-7281 was cofinanced by Fondo Europeo de Desarrollo Regional.

Acknowledgments

The authors would like to thank Dr. J.M. Garcia-Verdugo for supervision of electron microscopy procedures. We thank Elaine Lilly, PhD (Writer's First Aid), for English language revision.

References

Bellingham, M.C., Berger, A.J., 1996. Presynaptic depression of excitatory synaptic inputs to rat hypoglossal motoneurons by muscarinic M2 receptors. J. Neurophysiol. 76, 3758–3770.
Bodian, D., 1966. Electron microscopy: two major synaptic types on spinal motoneurons. Science 151, 1093–1094.
Carroll, R.C., Lissin, D.V., von Zastrow, M., Nicoll, R.A., Malenka, R.C., 1999. Rapid redistribution of glutamate receptors contributes to long-term depression in hippocampal cultures. Nat. Neurosci. 2, 454–460.
Castaneto, M.S., Gorelick, D.A., Desrosiers, N.A., Hartman, R.L., Pirard, S., Huestis, M.A., 2014. Synthetic cannabinoids: epidemiology, pharmacodynamics, and clinical implications. Drug Alcohol Depend. 144c, 12–41.
Castillo, P.E., Younts, T.J., Chavez, A.E., Hashimotodani, Y., 2012. Endocannabinoid signaling and synaptic function. Neuron 76, 70–81.
Chevaleyre, V., Takahashi, K.A., Castillo, P.E., 2006. Endocannabinoid-mediated synaptic plasticity in the CNS. Annu. Rev. Neurosci. 29, 37–76.
Crane, N.A., Schuster, R.M., Fusar-Poli, P., Gonzalez, R., 2013. Effects of cannabis on neurocognitive functioning: recent advances, neurodevelopmental influences, and sex differences. Neuropsychol. Rev. 23, 117–137.
Croxford, J.L., 2003. Therapeutic potential of cannabinoids in CNS disease. CNS Drugs 17, 179–202.
den Boon, F.S., Chameau, P., Schaafsma-Zhao, Q., van Aken, W., Bari, M., Oddi, S., Kruse, C.G., Maccarrone, M., Wadman, W.J., Werkman, T.R., 2012. Excitability of prefrontal cortical pyramidal neurons is modulated by activation of intracellular type-2 cannabinoid receptors. Proc. Natl. Acad. Sci. U. S. A. 109, 3534–3539.
Dobrunz, L.E., 2002. Release probability is regulated by the size of the readily releasable vesicle pool at excitatory synapses in hippocampus. Int. J. Dev. Neurosci. 20, 225–236.
Doze, V.A., Cohen, G.A., Madison, D.V., 1991. Synaptic localization of adrenergic disinhibition in the rat hippocampus. Neuron 6, 889–900.
El Manira, A., Kyriakatos, A., Nanou, E., Mahmood, R., 2008. Endocannabinoid signaling in the spinal locomotor circuitry. Brain Res. Rev. 57, 29–36.
Gonzalez-Forero, D., Montero, F., Garcia-Morales, V., Dominguez, G., Gomez-Perez, L., Garcia-Verdugo, J.M., Moreno-Lopez, B., 2012. Endogenous Rho-kinase signaling maintains synaptic strength by stabilizing the size of the readily releasable pool of synaptic vesicles. J. Neurosci. 32, 68–84.
Gonzalez-Forero, D., Portillo, F., Sunico, C.R., Moreno-Lopez, B., 2004. Nerve injury reduces responses of hypoglossal motoneurones to baseline and chemoreceptor-modulated inspiratory drive in the adult rat. J. Physiol. Lon. 557, 991–1011.
Gray, E.G., 1959. Axo-somatic and axo-dendritic synapses of the cerebral cortex: an electron microscope study. J. Anat. 93, 420–433.
Grundy, R.I., Rabuffetti, M., Beltramo, M., 2001. Cannabinoids and neuroprotection. Mol. Neurobiol. 24, 29–51.
Hall, W., Degenhardt, L., 2009. Adverse health effects of non-medical cannabis use. Lancet 374, 1383–1391.

Hirasawa, M., Schwab, Y., Natah, S., Hillard, C.J., Mackie, K., Sharkey, K.A., Pittman, Q.J., 2004. Dendritically released transmitters cooperate via autocrine and retrograde actions to inhibit afferent excitation in rat brain. J. Physiol. 559, 611–624.
Ho, J., Cox, J.M., Wagner, E.J., 2007. Cannabinoid-induced hyperphagia: correlation with inhibition of proopiomelanocortin neurons? Physiol. Behav. 92, 507–519.
Horner, R.L., 2007. Respiratory motor activity: influence of neuromodulators and implications for sleep disordered breathing. Can. J. Physiol. Pharmacol. 85, 155–165.
Kano, M., Ohno-Shosaku, T., Hashimotodani, Y., Uchigashima, M., Watanabe, M., 2009. Endocannabinoid-mediated control of synaptic transmission. Physiol. Rev. 89, 309–380.
Karila, L., Roux, P., Rolland, B., Benyamina, A., Reynaud, M., Aubin, H.J., Lancon, C., 2014. Acute and long-term effects of cannabis use: a review. Curr. Pharm. Des. 20, 4112–4118.
Kreitzer, A.C., Regehr, W.G., 2001. Retrograde inhibition of presynaptic calcium influx by endogenous cannabinoids at excitatory synapses onto Purkinje cells. Neuron 29, 717–727.
Laezza, C., Pisanti, S., Malfitano, A.M., Bifulco, M., 2008. The anandamide analog, Met-F-AEA, controls human breast cancer cell migration via the RHOA/RHO kinase signaling pathway. Endocr. Relat. Cancer 15, 965–974.
Lozovaya, N., Mukhtarov, M., Tsintsadze, T., Ledent, C., Burnashev, N., Bregestovski, P., 2011. Frequency-dependent cannabinoid receptor-independent modulation of Glycine receptors by endocannabinoid 2-AG. Front. Mol. Neurosci. 4, 13.
Maejima, T., Hashimoto, K., Yoshida, T., Aiba, A., Kano, M., 2001. Presynaptic inhibition caused by retrograde signal from metabotropic glutamate to cannabinoid receptors. Neuron 31, 463–475.
Mechoulam, R., Parker, L.A., 2013. The endocannabinoid system and the brain. Annu. Rev. Psychol. 64, 21–47.
Millar, A.G., Bradacs, H., Charlton, M.P., Atwood, H.L., 2002. Inverse relationship between release probability and readily releasable vesicles in depressing and facilitating synapses. J. Neurosci. 22, 9661–9667.
Montero, F., Portillo, F., Gonzalez-Forero, D., Moreno-Lopez, B., 2008. The nitric oxide/cyclic guanosine monophosphate pathway modulates the inspiratory-related activity of hypoglossal motoneurons in the adult rat. Eur. J. Neurosci. 28, 107–116.
Moreno-Lopez, B., Sunico, C.R., Gonzalez-Forero, D., 2011. NO orchestrates the loss of synaptic boutons from adult "sick" motoneurons: modeling a molecular mechanism. Mol. Neurobiol. 43, 41–66.
Morisset, V., Urban, L., 2001. Cannabinoid-induced presynaptic inhibition of glutamatergic EPSCs in substantia gelatinosa neurons of the rat spinal cord. J. Neurophysiol. 86, 40–48.
Mukhtarov, M., Ragozzino, D., Bregestovski, P., 2005. Dual Ca^{2+} modulation of glycinergic synaptic currents in rodent hypoglossal motoneurones. J. Physiol. 569, 817–831.
Navarrete, M., Araque, A., 2008. Endocannabinoids mediate neuron-astrocyte communication. Neuron 57, 883–893.
Ohno-Shosaku, T., Tsubokawa, H., Mizushima, I., Yoneda, N., Zimmer, A., Kano, M., 2002. Presynaptic cannabinoid sensitivity is a major determinant of depolarization-induced retrograde suppression at hippocampal synapses. J. Neurosci. 22, 3864–3872.
Peever, J.H., Shen, L., Duffin, J., 2002. Respiratory pre-motor control of hypoglossal motoneurons in the rat. Neuroscience 110, 711–722.
Pertwee, R.G., 2007. Cannabinoids and multiple sclerosis. Mol. Neurobiol. 36, 45–59.
Pertwee, R.G., 2010. Receptors and channels targeted by synthetic cannabinoid receptor agonists and antagonists. Curr. Med. Chem. 17, 1360–1381.
Rekling, J.C., Feldman, J.L., 1998. PreBotzinger complex and pacemaker neurons: hypothesized site and kernel for respiratory rhythm generation. Annu. Rev. Physiol. 60, 385–405.
Robbe, D., Alonso, G., Duchamp, F., Bockaert, J., Manzoni, O.J., 2001. Localization and mechanisms of action of cannabinoid receptors at the glutamatergic synapses of the mouse nucleus accumbens. J. Neurosci. 21, 109–116.
Roser, P., Gallinat, J., Weinberg, G., Juckel, G., Gorynia, I., Stadelmann, A.M., 2009. Psychomotor performance in relation to acute oral administration of Delta9-tetrahydrocannabinol and standardized cannabis extract in healthy human subjects. Eur. Arch. Psychiatry Clin. Neurosci. 259, 284–292.
Scanziani, M., Capogna, M., Gahwiler, B.H., Thompson, S.M., 1992. Presynaptic inhibition of miniature excitatory synaptic currents by baclofen and adenosine in the hippocampus. Neuron 9, 919–927.
Schikorski, T., Stevens, C.F., 2001. Morphological correlates of functionally defined synaptic vesicle populations. Nat. Neurosci. 4, 391–395.
Schneggenburger, R., Sakaba, T., Neher, E., 2002. Vesicle pools and short-term synaptic depression: lessons from a large synapse. Trends Neurosci. 25, 206–212.
Sullivan, J.M., 1999. Mechanisms of cannabinoid-receptor-mediated inhibition of synaptic transmission in cultured hippocampal pyramidal neurons. J. Neurophysiol. 82, 1286–1294.
Sunico, C.R., Dominguez, G., Garcia-Verdugo, J.M., Osta, R., Montero, F., Moreno-Lopez, B., 2011. Reduction in the motoneuron inhibitory/excitatory synaptic ratio in an early-symptomatic mouse model of amyotrophic lateral sclerosis. Brain Pathol. 21, 1–15.
Sunico, C.R., Gonzalez-Forero, D., Dominguez, G., Garcia-Verdugo, J.M., Moreno-Lopez, B., 2010. Nitric oxide induces pathological synapse loss by a protein kinase G-, Rho kinase-dependent mechanism preceded by myosin light chain phosphorylation. J. Neurosci. 30, 973–984.
Thakur, G.A., Nikas, S.P., Li, C., Makriyannis, A., 2005. Structural requirements for cannabinoid receptor probes. Handb. Exp. Pharmacol. 209–246.
Turkanis, S.A., Karler, R., 1983. Effects of delta 9-tetrahydrocannabinol on cat spinal motoneurons. Brain Res. 288, 283–287.
Turrigiano, G.G., Leslie, K.R., Desai, N.S., Rutherford, L.C., Nelson, S.B., 1998. Activity-dependent scaling of quantal amplitude in neocortical neurons. Nature 391, 892–896.
Uchizono, K., 1965. Characteristics of excitatory and inhibitory synapses in the central nervous system of the cat. Nature 207, 642–643.
van der Stelt, M., Veldhuis, W.B., Maccarrone, M., Bar, P.R., Nicolay, K., Veldink, G.A., Di Marzo, V., Vliegenthart, J.F., 2002. Acute neuronal injury, excitotoxicity, and the endocannabinoid system. Mol. Neurobiol. 26, 317–346.
Wiley, J.L., Marusich, J.A., Huffman, J.W., 2014. Moving around the molecule: relationship between chemical structure and in vivo activity of synthetic cannabinoids. Life Sci. 97, 55–63.
Zucker, R.S., 1989. Short-term synaptic plasticity. Annu. Rev. Neurosci. 12, 13–31.
Zucker, R.S., Regehr, W.G., 2002. Short-term synaptic plasticity. Annu. Rev. Physiol. 64, 355–405.